

INTERNATIONAL SOCIETY FOR SOIL MECHANICS AND GEOTECHNICAL ENGINEERING



This paper was downloaded from the Online Library of the International Society for Soil Mechanics and Geotechnical Engineering (ISSMGE). The library is available here:

<https://www.issmge.org/publications/online-library>

This is an open-access database that archives thousands of papers published under the Auspices of the ISSMGE and maintained by the Innovation and Development Committee of ISSMGE.

The effect of soil density on offshore wind turbine monopile foundation performance

S.M. Bayton & J.A. Black

Dept. of Civil and Structural Engineering, The University of Sheffield, Sheffield, United Kingdom

ABSTRACT: Centrifuge model tests were performed to evaluate the response of offshore wind turbine monopile foundations, in both loose and dense sand deposits, subjected to lateral loading at serviceability limit state (SLS). Model monopile experiments were performed at 100 gravities (100g) of a prototype pile of diameter 5 m embedded to a depth of 30 m ($L/D = 6$). Evolution of pile deflection, lateral force and pile bending moments were monitored. Comparison of the observed deflected shape and pile bending moments against $p - y$ methods of analysis predictions (API, 2011; DNV, 2014) indicate that design codes may underestimate the two parameters by up to 20 % at SLS. An initial series of 10 cycles at SLS were also carried out on the two sand densities. Results indicate an amount of ‘locked-in’ bending moment upon unload; a phenomenon which is more evident for the loose sand deposit.

1 INTRODUCTION

A strategic departure from traditional fossil fuel energy sources towards zero carbon electricity generation is necessary to lead to a sustainable, energy-independent society. The offshore wind energy sector presents a major opportunity to realize this, in particular in the United Kingdom, where offshore wind has the potential to meet the country’s demands three times over (Oswald *et al.*, 2008). Unfortunately, the industry is not expanding as rapidly as planned or required, as a result of a number of factors, none more so than the high capital investment of foundation material and installation. Improvement of foundation efficiency is one solution which would lead to an increased economic feasibility and greater deployment in the future.

The monopile is typically the preferred foundation solution today, with just under three quarters of all wind turbines founded on this type of structure. Owing to its simple and robust design, its suitability to mass-production and track record over the past decade, it is also likely to remain the leading foundation of choice for designers and contractors alike for water depths of proposed sites in the near future.

This paper presents the results from a suite of lateral loading tests at serviceability limit state (SLS) in the University of Sheffield’s 4m diameter 50g-tonne geotechnical beam centrifuge located in the Centre for Energy and Infrastructure Ground Research (CEIGR). The aim of the current research is to evaluate the effect of sand density on monopile performance and failure mechanism, subject to both monotonic and cyclic loading conditions. These are then

to be compared with traditional design code $p - y$ curve methods of analysis (API, 2011; DNV, 2014).

2 DESIGN CODE METHOD OF ANALYSIS

Over the design life of an offshore wind turbine, the structure’s foundation has to be able to withstand the harshest of weather conditions presented by the marine environments. The oil and gas industry has vast experience in managing these conditions. However, differences between the problems faced here and those encountered in the design of wind turbine foundations are significant; the most notable being the relatively large design lateral loads (F_h) applied to the wind turbine structure at great eccentricity (e) in comparison to the small vertical loads from the structure self-weight (as illustrated by Figure 1(a)).

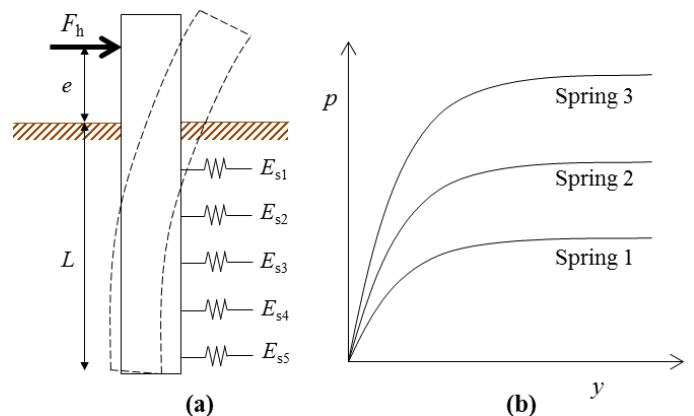


Figure 1. (a) Illustration of foundation spring approximation; (b) Non-linear $p - y$ curve spring foundation

Numerous methods of analysis exist to predict the behavior of piles in sand subjected to lateral loads. The subgrade reaction approximation theory, commonly known as the $p - y$ curve method of analysis, is one such method that is widely accepted by designers today, mainly due to its simple formulation and evaluation of results, as well as its reliable predictions throughout oil and gas industry history. Here, a spring model combined with non-linear soil property approximations form the backbone of current API (2011) and DNV (2014) design codes. The fundamental Euler-Bernoulli equation to describe pile deflected shape is as follows.

$$EI \frac{d^4 y}{dz^4} + Q_a \frac{d^2 y}{dz^2} - p(y) = 0 \quad (1)$$

where EI is the bending stiffness of the pile; y the horizontal deflection; z the depth below the seabed; Q_a the applied axial load (zero additional axial load was applied in these experiments); and $p(y)$ the soil resistance as a function of the horizontal deflection as defined by the $p - y$ curves in sand (Fig. 1(b)).

There are, however, concerns surrounding the translation of this design method to large-diameter wind turbine monopiles. Firstly, the fundamental foundation spring approximations, on which the method is formed, are based on empirically derived adjustment factors calibrated using experimental data obtained from piles of up to just 1.22 meters in diameter (O'Neill & Murchison, 1984). Significant questions over their validity are raised when extrapolating to today's monopiles, which already reach 7.5 meters in diameter, and expected to continue to increase in size.

One such concern extends to the different mechanisms of failure experienced by piles of different global stiffnesses. Monopile global stiffness is defined by both pile (bending stiffness, EI , and embedment length, L) and soil (elastic modulus, E_s) properties. Poulos & Hull's (1989) non-dimensional pile stiffness coefficient, K_r , proposed in Equation 2, suggests values for which global stiffness can be categorized.

$$K_r = \frac{E_s L^4}{EI} \quad (2)$$

where values less than 4.8 describe a perfectly rigid case, and greater than 388.6 perfectly flexible.

Traditional offshore piles for the oil and gas industry are typically classified as flexible and their failure is often governed by the realization of the bending resistance of the pile itself, with relatively little yielding of the surrounding soil. It is this type of failure mechanism that the fundamental empirical adjustment factors are based. This is in great contrast to typical monopile foundations for wind turbines, which can be considered rigid. Given the higher rigidity, these experience a combination of both rota-

tional and bending failure mechanisms, presenting significant complications to design.

Field scale and laboratory element experiments alongside comprehensive numerical finite element modelling (FEM) research is currently being carried out as part of the PISA (Pile Soil Analysis) project; the aim of which is to develop a new simple design methodology for large diameter monopile foundations. (Byrne *et al.*, 2015; Zdravkovic *et al.*, 2015). The framework for the proposed 1D finite model includes additional model springs to account for distributed moment along the pile, base shear and base moment resistance, with spring stiffnesses calibrated against FEM approximations. Initial results indicate a high consistency with the FEM approximation as well as the initial field scale tests. What remains to fully understand is the point of transition from traditional flexible $p - y$ curves to this new rigid approach, not just in terms of pile L/D ratios, but as global stiffness, K_r , including soil properties.

In addition to PISA, there have been several academic studies (Achmus *et al.*, 2005; Hamre *et al.*, 2011; Haiderali & Madabhushi, 2013), performed to investigate the rigid mechanism of failure, though these have concentrated on the variation of pile properties and not soil properties. In this respect, this paper reports on a series of centrifuge experimental large-diameter monopile foundation tests in sands of two different densities, loose and dense, to evaluate their effect on pile performance.

3 CENTRIFUGE EXPERIMENTAL METHOD

Offshore geotechnical engineering problems have been widely appraised using centrifuge modelling techniques; whether it is validation of design methods, verification of numerical predictions or simply to gain an insight into geotechnical design (Murff, 1996). The advantages of using centrifuge modelling techniques over traditional 1g techniques are numerous, none more so than the ability to recreate prototype soil stress conditions within the sample. This is paramount in evaluating the behavior of key mechanical properties of the soil, in particular within the small strain range, which cannot always be captured at lower confining stresses.

A series of centrifuge model tests, at a centrifugal acceleration of 100g, were conducted using the University of Sheffield's (UoS) 4m diameter 50g-tonne geotechnical beam centrifuge located in the Centre of Energy and Infrastructure Ground Research. The aim of these tests was to evaluate the structural response of monopile foundations at SLS embedded in sands of two different densities; loose and dense, and thus two different global system stiffness values (K_r). Table 1 provides details on the centrifuge.

Table 1. UoS 50g-tonne centrifuge specification

Description	Specification
Platform radius	2.0m
Payload size	W = 0.8 m (circumferential) L = 0.8 m (vertical in flight) H = 0.9 m (radial in flight)
Maximum acceleration	100g at 500kg payload, or 150g at 330kg payload

A fine grained sand commercially known as HST95 sand ($d_{50} = 0.2$ mm) was pluviated into the centrifuge strong box through a series of pre-calibrated meshes at a set drop height to give both loose and dense samples with relative densities (R_d) of 34 and 78 per cent respectively. Shear box tests revealed the angle of shear resistance to be 32 and 37.5° respectively. The cylindrical strong box had an internal diameter and height of both 500 mm, and provided a rigid boundary condition.

An aluminum pipe section with outer diameter 50 mm and wall thickness 2.8 mm was used throughout the test procedure to replicate a 5 m outer diameter pile. The wall thickness of the model pile (2.8 mm) was selected to reproduce the flexural stiffness (EI) of a typical steel monopile at prototype scale. Ten pairs of strain gauges (KFG type with gauge length 3 mm) in half bridge configurations were positioned on the pile extremity along its embedded length at 50 mm intervals. Bending moment calibration of the strain gauges was performed on each 90 degree orientation as well as in compression. Milled channels enabled routing of all wiring away from the strain gauges towards the top of the pile. Epoxy was positioned around these channels to protect the wiring. Protruding epoxy was then made flush with the curvature of the pile using fine sandpaper to preserve its original cylindrical profile. Figure 2 presents the arrangement of the model pile.

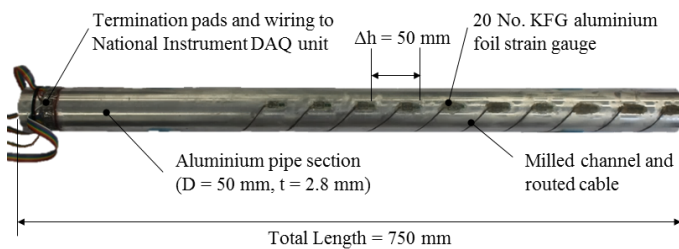


Figure 2. Model pile arrangement

The pile section was driven into position at 1g to an embedment depth of 30 meters prototype scale ($L/D = 6$). It is recognized here that pile driving at 1g does not provide a full representation of the *in situ* stresses that will develop around the pile. In fact, Dyson and Randolph (2001) suggest a 20 – 30 % increase in ultimate lateral capacity for in-flight driving, similarly observed by Klinkvort *et al.* (2013). This needs to be therefore taken into consideration when analyzing the experimental results. Table 2 defines the pile configuration.

Table 2. Pile configuration – model and prototype scale

Description	Model Dimension	Prototype Dimension
Diameter (D)	50 mm	5.0 m
Thickness (t)	2.8 mm	84 mm
Material	Aluminum	Steel
Young's Modulus (E)	69 GPa	205 GPa
Flexural Stiffness (EI)	$8.01 \times 10^3 \text{ Nm}^2$	$8.01 \times 10^{11} \text{ Nm}^2$
Bending Resistance (M_{rd})	1120 Nm	650 MNm
Embedment Length (L)	300 mm ($L/D = 6$)	30.0 m
K_r (Dense Sand)	64 (Transition)	
K_r (Loose Sand)	34 (Transition)	

A loading frame was assembled to ensure that the lateral load was applied at the highest possible location in relation to the dimensional constraints of the centrifuge payload. This allowed for the ratio of applied lateral load to overturning moment at the seabed to be as close to prototype as possible ($z/D = 6$), best replicating *in situ* loading conditions. It is however noted that the load eccentricity is not a complete representation of prototype conditions since this is closer to the location of wave loading rather than an overall wind and wave combination.

Load application was achieved by the use of an 80 mm diameter dual acting pneumatic cylinder actuator, with a maximum load capacity of 5.0 kN [50 MN at 100g]. A load cell calibrated over the range of 2.5 kN was attached to the end of the actuator piston that interfaced to the pile. Two linear variable differential transformers (LVDT) were attached to the frame to give values of horizontal displacement. These readings, alongside the bending moment readings from the strain gauges, were necessary to compute the deflected shape by double integration. Figure 3 presents the experimental setup.

Lateral load was applied until the theoretical bending resistance at prototype scale of the steel pile was reached ($M_{rd,p} = 650$ MNm, equivalent to 650 Nm at model scale). This was taken to be the ultimate limit state (ULS) for the collective pile-soil system.

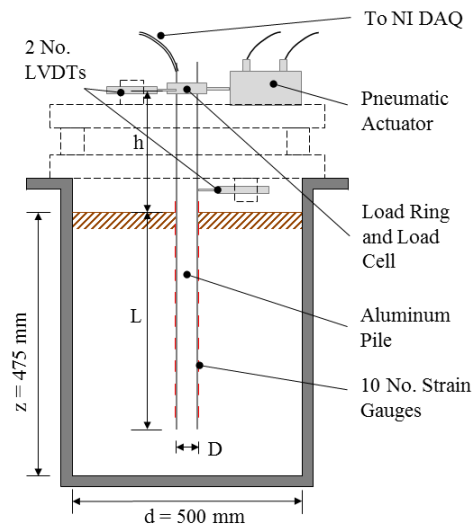


Figure 3. Centrifuge lateral loading frame experimental setup

4 MONOTONIC LOADING

The lateral load, F_h , displacement, y , relationships observed for both the loose and dense sample are plotted using prototype units in Figure 4. The lateral displacement measurement presented is referenced at the mudline and is normalized by the diameter of the pile (D). As a point of interest, the lateral load at serviceability limit state (SLS), defined as 50% of the ultimate limit state (ULS) load (DNV, 2014) for the loose sample is also marked on Figure 4. It is clear that for a soil with greater density, the deflection experienced for the same magnitude of applied load is much less than that of the loose sample. This is echoed in the stiffness response observed, where the dense sample produces a stiffer response.

In addition, it can be seen that for the dense sample, the load-deflection evolves linearly; suggesting that minimal global yielding of the soil has taken place. There may be an amount of localized yielding, particularly at the pile surface and toe, though this has minimal effect on global pile resistance. In reality, failure is governed by excessive bending of the pile itself. For the loose sample on the other hand, there is an indication that a degree of plastic deformation of the soil has taken place. This supports the hypothesis that for higher global pile stiffnesses (lower values of K_r parameter), in this case due to a reduced E_s value from a looser sample, the mechanism is indeed towards a rotation failure and plastic yielding of the surrounding soil.

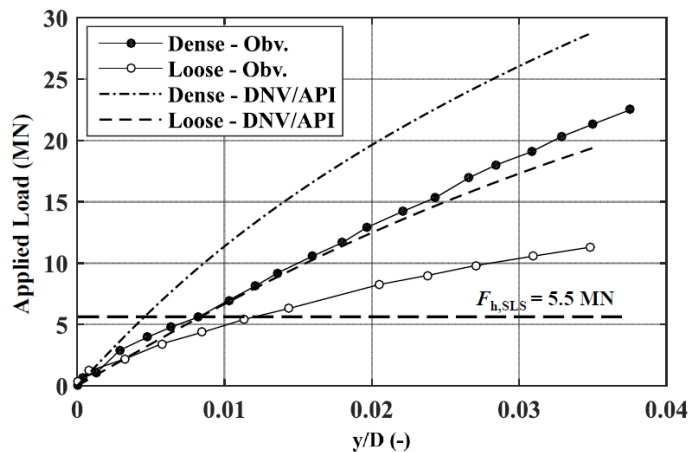


Figure 4. Lateral load – displacement response observed

Comparison with current design code recommendations suggests that there is an over prediction of pile capacity for loads within the range tested. This observation agrees with the initial finite element modelling (FEM) results obtained from the PISA project (Byrne *et al.*, 2015) whereby results show design codes also over predicting the soil resistance in sand, in particular for short piles in the range tested. It is worth noting that by driving the pile in flight, it would be expected that the pile would experience a stiffer response as well as greater ultimate

capacity, and therefore be closer to the design code recommendation. It would have also been useful to continue the loading further to allow for substantial soil yielding to occur, and therefore allow further comparison with design code and PISA predictions, however in this case the prototype pile bending resistance would have been reached.

Evolution of the moments to serviceability limit state for both sand densities is presented in Figure 5. Note zero on the vertical z/D axis corresponds to the sea bed surface.

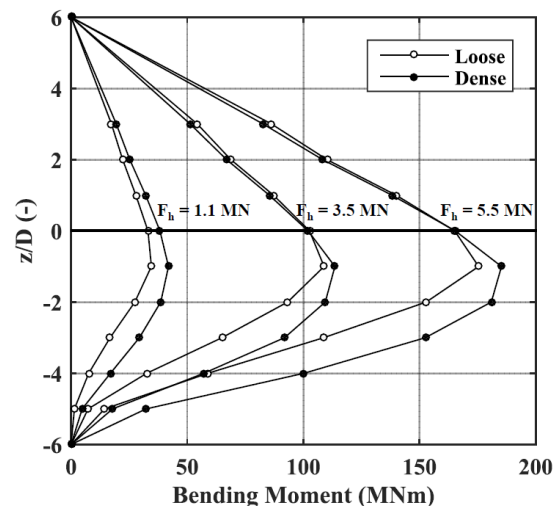


Figure 5. Evolution of bending moment with successive applied load to serviceability limit state ($F_{h,SLS} = 5.5$ MN)

It is clear that the general shape of the bending moment diagrams for each density is consistent, suggesting that the overall behavior of the soil-pile interaction at each density is similar. The piles can also be classified as non-slender given the absence of a point of inflexion on the bending moment diagram. Comparison the two sand densities shows that the maximum bending moment below the soil surface is greater for the dense sand. This supports the idea that a pile system with a higher global pile-soil stiffness parameter, K_r , fails with increased bending in relation to soil yielding. In addition, the loose sample experiences less bending for a greater deflection and therefore must be accounted for by rotation and soil yielding.

Finally, with the aid of MATLABTM programming software, the current design code $p - y$ curve method of analysis, was evaluated for the two pile and soil configurations, and compared with observed pile deflected shape. From Figure 6, it can be seen that there is a similarity in the predicted and observed deflected shape general form, in terms of rotation, bending and toe-kick. However, in both cases, the rotation at the seabed and the resulting deflections are underestimated by up to 20 per cent. This observed softer response for SLS loads is also observed by the FEM and field scale tests of the PISA project

(Byrne *et al.*, 2015) as well as FEM studies in sand carried out in Germany (Achmus *et al.*, 2005).

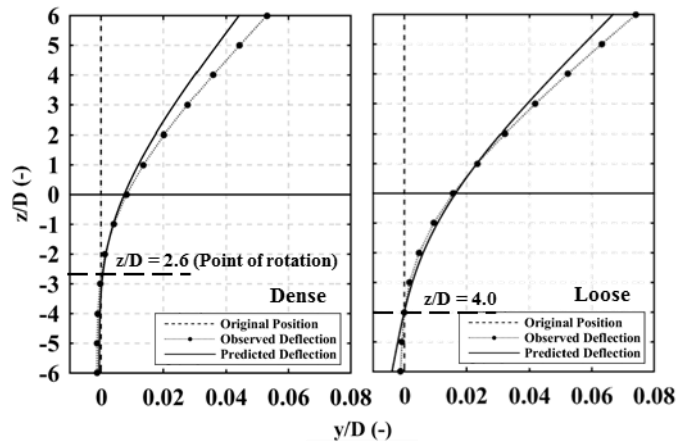


Figure 6. Comparison of observed and predicted deflected shape at serviceability limit state ($F_h = 5.5$ MN)

From further observation, it can also be seen that for the denser sand, the depth to which the pile experiences the point of rotation is much closer to the seabed in comparison with the loose sample ($z/D = 2.6$ compared to $z/D = 4.0$). This is intuitive since a denser sample provides greater lateral and rotational restraint and emulates more an encastre support condition; another reason for the greater bending moment experienced below the soil surface in comparison to the loose deposit.

The underestimation of deformation and resulting bending moments by the $p - y$ method may be attributed to the high levels of empiricism within the code not allowing for accurate extrapolation to monopiles with such large diameters or global stiffnesses. Based on this current set of experimental results, alongside previous literature observations, it would be inappropriate to assume that the current $p - y$ design methods provide reasonable predictions for large-diameter monopile foundations. The initial available results from the proposed PISA 1D finite code recommendation show very promising results for the development of an accurate design method for rigid, large-diameter monopiles, though the details of this method, in terms of model development and spring stiffnesses is yet to be disclosed. Once available, it will be necessary validate this proposed method for a range of pile-soil stiffness scenarios, with centrifuge modelling being an ideal platform to provide an economical method of realizing this.

5 BASIC CYCLIC LOADING

Given the small extent of global yielding experienced in the initial monotonic loading phase of the experiments, it was thought beneficial to further utilize the setup whilst the centrifuge was in operation to carry out additional investigation into the effects of sand density on the pile behavior subjected to a

small number of cyclic loads. It is to be admitted that the pile and sample had already been loaded to a level greater than predicted serviceability limit state load, and as such this cyclic loading series was not carried out on a virgin sample. In addition only 10 one way cycles, using a load controlled sinusoidal function with a period of 20 seconds, were applied at SLS ($F_h = 5.5$ MN). This is well below the current maximum of 1000 cycles in a centrifuge environment in published literature (Kirkwood & Haigh, 2014). The aim of these 10 cycles was, therefore, to simply provide the authors with an indication of general behavior with future testing in mind and provide validation of previous literature observations. The results do offer some additional benefit, since cyclic lateral loading in different sand densities has not been previously performed in an elevated gravity, and as such these will give insight into the effect of soil properties on pile behavior evolution.

Unfortunately there is no scope for comparing the stiffness evolution with cycles of the two different densities, since the loose sample data for pile deflection cannot be presented due to a malfunction with the LVDTs. The problem was later rectified for the dense sample test. The effect of soil density on the evolution of bending moments developed within the pile with cycles can, however, be evaluated.

Upon each cyclic application of load, it can be seen (Fig. 7a) that the maximum moment experienced within the pile reduces. When the load was removed, the bending moment did not return to zero and a residual 'locked-in' bending moment was observed (Fig. 7b); increasing with cycle number. This phenomenon of 'locked-in' bending moments has also been observed in cyclic experiments by Kirkwood & Haigh (2013). It can be suggested that pile movement allows a redistribution and flow of sand on each cycle preventing gapping behind the pile, and thus changes in soil stiffness are experienced. This results in a 'locked-in' internal bending moment within the pile owing to the new soil-structure interaction regime established. This hypothesis should be validated with *in situ* soil measurements and observational techniques.

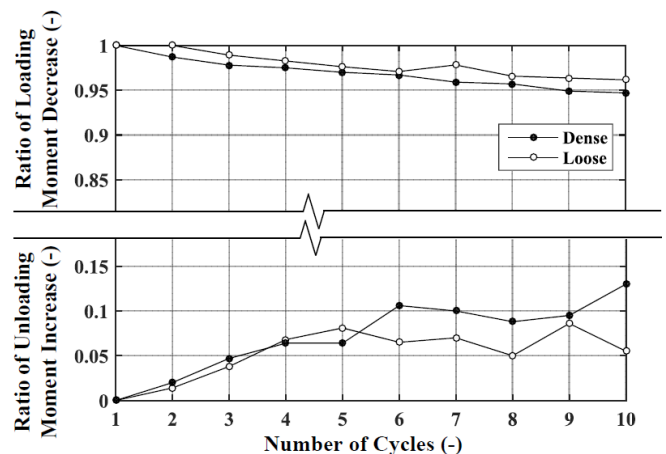


Figure 7. Evolution of maximum on loading (top) and residual on unloading (bottom) bending moments with number of cycles

Figure 8 presents the loaded and unloaded bending moments after 10 cycles for both dense and loose soil samples. It is clear that the pile embedded in dense sand retains a much lower ‘locked-in’ bending moment (approximately 12 % retained for the dense sample compared with 35 % for the loose). This difference indicates that for a dense sample, there is significantly less redistribution of sand in comparison to the loose sample. It may be suggested that the lower void ratio of dense sand results in a lower availability for sand particles to move.

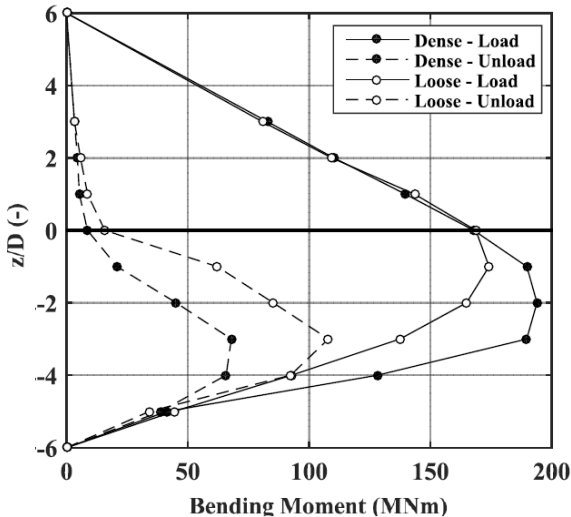


Figure 8. ‘Locked-in’ bending moment phenomenon on load and unload after 10 cycles ($F_h = 5.5$ MN)

Upon spindown of the centrifuge, when the elevated stress field in the soil reduces, the ‘locked-in’ moments dissipated, confirming that this was indeed an increased horizontal confining stress within the soil restraining the monopile on unload.

6 CONCLUSION

A series of centrifuge modelling experiments has been carried out evaluating the behavior of wind turbine monopile foundations subjected to serviceability limit state loads in two densities of sand. Comparison of observed and predicted deflected shapes (using the $p - y$ method) show an underestimation of up to 20 % of the design code pile deflection as well as the consequential flexural bending moments, agreeing with previous literature observations.

A series of 10 cycles at SLS were also carried out. Upon each cyclic application of load, the maximum moment experienced within the pile reduced. On unload, an amount ‘locked-in’ bending moment was also observed, owing to a potential new soil-structure interaction regime established. For a pile embedded in dense sand, on unload, a much lower proportion of the maximum bending moment is experienced indicating that, there is significantly less redistribution of sand in comparison to the loose sample.

7 REFERENCES

- Achmus, M., Abdel-Rahman, K. & Peralta, P., 2005. On the Design of Monopile Foundations with Respect to Static and Quasi-Static Cyclic Loading, *Copenhagen Offshore Wind*, 2005
- American Petroleum Institute (API), 2011. *RP 2A-WSD Recommended Practice for Planning, Designing and Constructing Fixed Offshore Platforms – Working Stress Design, 21st Edition*. Washington, USA
- Byrne, B.W., McAdam, R., Burd, H.J., Houlsby, G.T., Martin, C.M., Zdravković, L., Taborda, D.M.G., Potts, D.M., Jardine, R.J., Sideri, M., Schroeder, F.C., Gavin, K., Doherty, P., Igoe, D., Muir Wood, A., Kallehave, D. & Skov Gretlund, J., 2015. New design methods for large diameter piles under lateral loading for offshore wind applications. *3rd ISFOG, 2015*, Oslo, Norway
- Det Norske Veritas AS (DNV), 2014. *DNV-OS-J101 Design of Offshore Wind Turbine Structures*
- Dyson, G.J. & Randolph, M.F., 2001. Monotonic lateral loading of piles in calcareous sand, *Journal of Geotechnical and GeoEnvironmental Engineering*, Vol. 127, No. 4, pp. 346 – 352
- Haiderali, A.E. & Madabhushi, G.S.P., 2013. Evaluation of the $p - y$ Method in the Design of Monopiles for Offshore Wind Turbines. In: *Proceedings from the Offshore Technology Conference*, Texas, USA, 6-9 May, pp. 1824-1844
- Hamre, L., Feizi Khankandi, S., Strom, P.J. & Athanasiu, C., 2011. Lateral Behaviour of Large Diameter Monopiles at Sheringham Shoal Wind Farm. *Frontiers in Offshore Geotechnics II*. Gourvenec & White, London
- Kirkwood, P.B. & Haigh, S.K., 2014. Centrifuge Testing of Monopiles subject to Cyclic Lateral Loading. *Physical Modelling in Geotechnics*, pp.827-831
- Klinkvort, R.T., Heddal, O. & Springman, S., 2013. Scaling issues in centrifuge modelling of monopiles, *International Journal of Physical Modelling in Geotechnics*, Vol. 13, No. 2, pp. 38 – 49
- Murff, J.D., 1996. The Geotechnical Centrifuge in Offshore Engineering. *Offshore Technology Conference*, OTC 8265
- O’Neill, M.W. & Murchison, J.M., 1984. Evaluation of $p-y$ Relationships in Cohesionless Soils. In: *Analysis and Design of Pile Foundations. Proceedings of a Symposium in Conjunction with the ASCE National Convention*, pp. 174-191
- Oswald, J., Raine, M. & Ashraf-Ball, H., 2008. *Will British Weather Provide Reliable Electricity? Energy Policy*, Vol. 36, pp. 3212-3225
- Poulos, H. & Hull, T., 1989. The Role of Analytical Geomechanics in Foundation Engineering. *Foundation Engineering: Current Principles and Practices*, Vol. 2, pp. 1578–1606
- Zdravković, L., Taborda, D.M.G., Potts, D.M., Jardine, R.J., Sideri, M., Schroeder, F.C., Byrne, B.W., McAdam, R., Burd, H.J., Houlsby, G.T., Martin, C.M., Gavin, K., Doherty, P., Igoe, D., Muir Wood, A., Kallehave, D. & Skov Gretlund, J., 2015. Numerical modelling of large diameter piles under lateral loading for offshore wind applications. *3rd ISFOG*, Oslo, Norway